and helpful conversations with P. Green, C. J. Palmstrøm, W. W. Graessley, B. Crist, H. Sillescu, and J. Klein. We found the preprint of his paper outlining a theory of ring reptation, kindly provided by Klein, to be particularly useful.

Registry No. PS, 9003-53-6.

References and Notes

(1) Klein, J. *Nature (London)* **1978**, *271*, 143.
(2) Klein, J. *Macromolecules* **1981**, *14*, 460; *Philos. Mag.* **1981**, *43*, 771.
(3) Antonietti, M.; Coutandin, J.; Gruetter, R.; Sillescu, H. *Macromolecules* **1984**, *17*, 798.
(4) Smith, B. A.; Samulski, E. T.; Yu, L.-P.; Winnik, M. A. *Phys. Rev. Lett.* **1984**, *52*, 45.
(5) Green, P. F.; Mills, P. J.; Palmstrøm, C. J.; Mayer, J. W.; Kramer, E. J. *Phys. Rev. Lett.* **1984**, *53*, 2145.
(6) Mills, P. J.; Green, P. F.; Palmstrøm, C. J.; Mayer, J. W.; Kramer, E. J. *Appl. Phys. Lett.* **1984**, *45*, 957.
(7) Antonietti, M.; Coutandin, J.; Sillescu, H. *Makromol. Chem., Rapid Commun.* **1984**, *5*, 525.
(8) de Gennes, P.-G. *J. Chem. Phys.* **1971**, *55*, 572.
(9) Edwards, S. F. *Molecular Fluids*; Balian, R., Weill, G., Eds.; Gordon and Breach: London, 1976; p 155.
(10) de Gennes, P.-G. *Scaling Concepts in Polymer Physics*; Cornell University: Ithaca, NY, 1979; p 219.
(11) Graessley, W. W. *Adv. Polym. Sci.* **1982**, *47*, 67.
(12) Klein, J. *Macromolecules* **1978**, *11*, 852.
(13) Daoud, M.; de Gennes, P.-G. *J. Polym. Sci., Polym. Phys. Ed.* **1979**, *17*, 1971.
(14) Klein, J. *Polym. Prepr. (Am. Chem. Soc., Div. Polym. Chem.)* **1979**, *22*, 105.
(15) Klein, J.; Fletcher, D.; Fetters, L. J. *Nature (London)* **1983**, *304*, 526.
(16) Fletcher, D. P.; Klein, J. *Polym. Comm.* **1985**, *26*, 2.
(17) Bartels, C. R.; Crist, B.; Fetters, L. J.; Graessley, W. W. *Macromolecules* **1986**, *19*, 785.
(18) de Gennes, P.-G. *J. Phys. (Les Ulis, Fr.)* **1975**, *36*, 1199.
(19) Doi, M.; Kuzuu, N. Y. *J. Polym. Phys., Polym. Lett. Ed.* **1980**, *18*, 775.
(20) Klein, J.; Fletcher, D.; Fetters, L. J. *Faraday Symp. Chem. Soc.* **1983**, *18*, 159.
(21) Needs, R. J.; Edwards, S. F. *Macromolecules* **1983**, *16*, 1492.
(22) Marrucci, G. *Adv. Transport Processes* **1984**, *5*.
(23) Pearson, D. S.; Helfand, E. *Faraday Symp. Chem. Soc.* **1983**, *18*, 189.
(24) Klein, J. *Macromolecules* **1986**, *19*, 105.
(25) Hild, G.; Kohler, A.; Rempp, P. *Eur. Polym. J.* **1980**, *16*, 525.
(26) Hild, G.; Strazielle, C.; Rempp, P. *Eur. Polym. J.* **1983**, *19*, 721.
(27) McKenna, G. B.; Hadziioannou, G.; Lutz, P.; Hild, G.; Strazielle, C.; Straupe, C.; Rempp, P.; Kovacs, A. *Macromolecules* **1987**, *20*, 498.
(28) Lutz, P.; Strazielle, C.; Rempp, P. *Polym. Prepr. (Am. Chem. Soc., Div. Polym. Chem.)* **1986**, *27*(1), 190.
(29) Hadziioannou, G.; Cotts, P.; ten Brinke, G.; Han, C.; Lutz, P.; Strazielle, C.; Rempp, P.; Kovacs, A. *Macromolecules* **1987**, *20*, 493.
(30) Geiser, D.; Höcker, H. *Macromolecules* **1986**, *13*, 653.
(31) Geiser, D.; Höcker, H. *Polym. Bull. (Berlin)* **1980**, *2*, 591.
(32) Vollmert, B.; Huang, J. *Makromol. Chem., Rapid. Commun.* **1980**, *1*, 333; **1981**, *2*, 467.
(33) Höcker, H. *Angew. Makromol. Chem.* **1981**, *87*, 100.
(34) Roovers, J.; Toporowski, P. M. *Macromolecules* **1983**, *16*, 843.
(35) ten Brinke, G.; Hadziioannou, G. *Macromolecules* **1987**, *20*, 480.
(36) Green, P. F.; Mills, P. J.; Kramer, E. J. *Polymer* **1986**, *27*, 1063.
(37) Doyle, B. L.; Peercy, P. S. *Appl. Phys. Lett.* **1979**, *34*, 811.
(38) Turos, A.; Meyer, O *Nucl. Instrum. Methods* **1984**, *232*, 92.
(39) Chu, W.-K.; Mayer, J. W.; Nicolet, M. A. *Backscattering Spectrometry*; Academic: New York, 1978.
(40) Kennedy, E. F., unpublished.
(41) Ziegler, J. F. *The Stopping and Ranges of Ions in Matter*; Pergamon: New York, 1977; Vol. 4. Anderson, H. H.; Ziegler, J. F. Ibid., Vol. 3.
(42) Crank, J. *The Mathematics of Diffusion*, 2nd ed.; Oxford University: Oxford, 1975; p 15.
(43) The authors also reported a $D^* < 1 \times 10^{-14}$ cm^2/s when the same *M*-ring/*P*-chain sample was prepared by slowly evaporating the solvent. They now attribute this result to association of the fluorescent labels during this treatment; Sillescu, H., private communication.
(44) Klein 24 argues that under certain conditions only not all the *P*-chain constraints along an *M*-chain can be independent; i.e., reptation of one *P*-chain releases more than one constraint. His idea leads to $D_{CR} \sim P^{-5/2}$, for which there is also some experimental support; Montfort, J. P.; Marin, G.; Monge, G. *Macromolecules* **1984**, *17*, 1551. Green, P. F.; Kramer, E. J. *Macromolecules* **1986**, *19*, 1108. Using a $P^{-5/2}$ law instead of the P^{-3} law for constraint release does not improve the agreement between theory and experiment for ring diffusion.
(45) Antonietti, M.; Sillescu, H. *Macromolecules* **1986**, *19*, 798.
(46) Roovers, J. *Macromolecules* **1985**, *18*, 1359.

Intrinsic Viscosity and Huggins Coefficients for Potassium Poly(styrenesulfonate) Solutions

R. M. Davis† and W. B. Russel*

Department of Chemical Engineering, Princeton University, Princeton, New Jersey 08544.
Received June 30, 1986

ABSTRACT: The intrinsic viscosities $[\eta]$ and Huggins coefficients k_H measured for potassium poly(styrenesulfonate) solutions at ionic strengths of (3×10^{-5})–3.1 M illustrate the effects of intra- and intermolecular electrostatic interactions on the viscosity of dilute solutions. With decreasing ionic strength $[\eta]$ increases monotonically as the individual chains transform from compact coils to extended rods, but k_H first decreases due to coil compression before increasing substantially. Extant theories predict the variation in $[\eta]$ satisfactorily but not the behavior of k_H.

Introduction

This paper is the second of two dealing with the thermodynamics and rheology of dilute polyelectrolyte solutions. The first[1] outlined an electrostatic wormlike chain theory, based on the earlier work of Odijk[2-4] and Fixman,[5-7] for thermodynamic properties such as the radius of gyration R_g and the second virial coefficient A_2. We then combined this with the hydrodynamic wormlike chain theory of Yamakawa[8] to predict the intrinsic viscosity $[\eta]$ and the molecular friction factor f_0. The theory was tested with light scattering and viscometry data for potassium poly(styrenesulfonate) K-PSS).[9] Agreement was quantitative for the thermodynamic properties and semiquantitative for the hydrodynamic predictions.

To test this theory further we have conducted viscometric experiments on a series of well-characterized K-PSS samples with a narrow molecular weight distribution over a range of ionic strengths encompassing the rigid-rod and

†Current address: Hercules, Inc., Research Center, Wilmington, DE 19899.

0024-9297/87/2220-0518$01.50/0

Gaussian coil limits. The resulting data for $[\eta]$ and the Huggins coefficient k_H, defined in the virial expansion for the solution viscosity, η

$$\eta_r = \eta/\eta_0 = 1 + [\eta]c + k_H[\eta]^2c^2 + \mathcal{O}(c^3) \quad (1)$$

with η_0 the solvent viscosity and c the polymer concentration, clearly demonstrate the strong effect of ionic strength on intra- and intermolecular interactions.

A survey of the literature reveals no other studies combining viscometry with the requisite light scattering measurements. The data for monodisperse K-PSS from Raziel and Eisenberg[9] did not extend far from the Gaussian coil limit. However, the close agreement of our predictions for R_g and A_2 with their measurements[1] gives us confidence in extending the calculations to the lower ionic strengths of this study. The combination of experiment and theoretical interpretation delineates the effect of the random coil to extended rod transition on $[\eta]$ and the associated nonmonotonic variation in k_H produced by intermolecular interactions. Before describing the experimental work, we summarize the theory for a wormlike chain molecule.

Review of Theory

Electrostatic Wormlike Chain Theory. The theory characterizes a polyelectrolyte in solution as a continuous filament with radius a, contour length L, persistence length $L_p = L_K/2$ (L_K is the Kuhn length), and a smoothed charge density equivalent to an average spacing L_c between charges. Intramolecular interactions are separated into those between nearby portions of the backbone, which determine the persistence length, and those between distant portions of the chain, accounted for through the binary cluster integral β. Polyelectrolytes, therefore, expand through two mechanisms since reducing the ionic strength increases both the persistence length and the binary cluster integral.

Representing the electrostatic contribution to the persistence length as

$$L_p = L_\infty + \hat{G}(a\kappa, L_B/L_c)/4\kappa^2L_B \quad (2)$$

with L_∞ the persistence length of uncharged backbone, κ^{-1} the Debye length, and L_B the Bjerrum length, defines $\hat{G}$ as the correction to the original theory[17] which calculates L_p from solutions to the linearized Poisson–Boltzmann equation about a line charge. For $L_B/L_c > 1$ and $a\kappa \leq 0.1$, $\hat{G} \sim 0.5$–1.0 but $\hat{G} \gg 1$ for $a\kappa \geq 1$. The radius of gyration for the wormlike chain without excluded volume then follows from[10]

$$R_{g0}^2 = L^2\left(\frac{1}{6N_k} - \frac{1}{4N_k^2} + \frac{1}{4N_k^3} - \frac{1 - e^{-2N_k}}{8N_k^4}\right) \quad (3)$$

with $N_k = L/L_K$. Note that

$$\lim_{N_k\to\infty} R_{g0}^2 = \frac{L^2}{6N_k}$$

$$\lim_{N_k\to 0} R_{g0}^2 = \frac{L^2}{12}$$

corresponding to the Gaussian coil and rigid-rod limits. Thus as the ionic strength decreases, the persistence length increases, causing the coil to expand.

Characterizing the addition coil expansion due to excluded volume requires the binary cluster integral β[10] for interactions between rods with length $2L_p$. Decomposing the integral as

$$\beta = \beta_c + \beta_e + \beta_a \quad (4)$$

distinguishes the contributions from the hard core

$$\beta_c = \pi a L_K^2$$

and the electrostatic interactions[6]

$$\beta_e = (2L_K^2/\kappa)R(w) \quad (5)$$

with

$$w = \frac{2\pi}{L_B\kappa}\left\{\left(\frac{L_B}{L_c}\right)_{eff}\frac{1}{a\kappa K_1(a\kappa)}\right\}^2 e^{-2a\kappa}$$

$R(w)$ is a function tabulated by Fixman and Skolnick,[6] and K_1 is the modified Bessel function of the first kind. The contribution from attractions, β_a, is added to account for the existence of a Θ or ideal state with $\beta = 0$.

The corresponding excluded volume parameter, derived for a worklike chain by Yamakawa and Stockmayer[11] as

$$z = \frac{3}{4}\left(\frac{3}{2\pi}\right)^{3/2} N_k^{1/2}\frac{\beta}{L_K^3}K(N_k) \equiv z_\infty K(N_k) \quad (6)$$

accounts for both the strength of the segment–segment interaction, embodied in β, and the probability of intramolecular contacts through the function $K(N_k)$. Note that

$$\lim_{N_k\to\infty} K(N_k) = 4/3$$

$$\lim_{N_k\to 0} K(N_k) = 0$$

indicating that $z \to 0$ and excluded volume effects become less important for stiff chains because distant segments along the chain rarely encounter one another. The chain expansion factor[12]

$$\alpha = [0.541 + 0.459(1 + 6.04z)^{0.46}]^{1/2} \quad (7)$$

associated with the excluded volume, together with the chain stiffening in eq 3, then determines the radius of gyration as

$$R_g = \alpha R_{g0} \quad (8)$$

Figures in our earlier paper[1] compile the requisite functions from the original sources, $\hat{G}$ (Figure 3), $\hat{R}$ (Figure 5), $(L_B/L_c)_{eff}$ (Figure 2), β_a (Figure 7), and K (Figure 4).

Hydrodynamics of Wormlike Chains. Existing theories for the hydrodynamics of wormlike chains[8] account for stiffness through L_p but not for the effect of excluded volume. To incorporate the latter in an approximate fashion we renormalize the persistence length to L_p' ($= L_K'/2$) to preserve the correct radius of gyration as

$$R_{g0}(L, N_k') = \alpha(z)R_{g0}(L, N_k) \quad (9)$$

with $N_k' = L/L_K'$. Then the existing results determine the intrinsic viscosity as

$$[\eta] = (L^{3/2}/M)g(N_k', a/L_p') \quad (10)$$

with g known numerically.[8] The limits

$$\lim_{N_k'\to\infty} [\eta] = \Phi_\infty\frac{N_k'^{3/2}L_K'^3}{M}$$

$$\lim_{N_k'\to 0} [\eta] = \frac{\pi N_A L^3}{24M(\ln(L/2a) - 0.9471)}$$

correspond to known results for Gaussian coils and rigid rods. Here $\Phi_\infty = 2.87 \times 10^{23}$ mol^{-1}, N_A is Avogadro's number, and M is the molecular weight.

Huggins Coefficient. Several theories predict the Huggins coefficient, characterizing the effect of pair interactions on the viscosity, under specific limiting condi-

Table I
Polymer Characterization Data[a]

sample no.	PS M_w	M_w/M_n	DP	L, nm	% sulfonation exptl	% sulfonation quoted	K-PSS M	L_B/L_c
24	20.4	1.06	196	49.4	0.91	0.88	41.5	2.58
25	53.7	1.05	516	130.0	0.92	0.89	109.5	2.61
17	598.8	1.05	5750	1449.0	0.86	0.76	1170.0	2.44

[a] Monomer length L_s = 0.252 nm; backbone radius a = 0.5 nm; Θ-state persistence length L_∞ = 1.4 nm; parameter in attractive potential A = −2.86 nm^4.

tions. For example, Batchelor[13] calculated $k_H = 0.99$ for hard spheres while Saito[14] and Freed and Edwards[15] found $k_H = 0.40$ for free-draining coils and $k_H = 0.76$ for non-draining coils. The treatment of excluded volume is difficult though.

Excluded volume affects the Huggins coefficient in two distinct ways. The decrease in the radius of gyration with increasing concentration in a good solvent contributes a negative term while the direct intermolecular interactions generate a positive term, analogous to the second virial term in the osmotic pressure. The treatment of Muthukumar and Freed[16] incorporates both for $z \ll 1$ as

$$k_H = k_{H\theta}(1 + Az) - (B/[\eta]_\theta)z + \mathcal{O}(z^2) \qquad (11)$$

Here the subscript θ implies $\lim_{z\to 0}$ and A and B are unknown functions of molecular weight, representing the direct interaction and coil compression effects, respectively. Understanding of these functions appears to be limited though.

The analysis of Russel[17] assumes a smoothed segment density, ignoring the effect of interactions on the coil conformation. The results suggest that for free-draining coils the Huggins coefficient should vary as

$$k_H = 0.40 + \frac{6\pi\eta_0 R_g}{f_0} f(\bar{z}) \qquad (12)$$

with $\bar{z} = z_\infty/\alpha^{3/2}$ and $f(\bar{z})$ a known function.

For small excluded volume $f(\bar{z}) \sim 2.62\bar{z}^2$, corresponding to the higher order terms in (11). Though f increases monotonically with $\bar{z}$, the complex dependence on κ, α, and R_g does not translate into a monotonic increase with decreasing ionic strength as we shall see later.

Experimental Techniques

Solution Preparation. Three different molecular weights of partially sulfonated poly(styrenesulfonate) (Na-PSS) purchased from the Pressure Chemical Co. (Pittsburgh) were converted to potassium poly(styrenesulfonate) (K-PSS) by dialysis with nitric acid and then deionized water. The resulting poly(styrenesulfonic acid) was neutralized to K-PSS at pH 7 by using reagent grade potassium hydroxide. We monitored the progress of the titration with an Orion glass combination electrode. After a pH of 7.0 ± 0.05 was reached and maintained for more than 2 min, the volume of titrant was recorded and the titration ended. The titration was performed under nitrogen to prevent absorption of atmospheric CO_2.

Pressure Chemical provided values for the weight- and number-average molecular weights M_w and M_n of the parent polystyrene stocks, the polydispersity index (M_w/M_n) of the Na-PSS based on GPC analysis, and the degree of sulfonation, d, of the polymer based on X-ray fluorescence tests. Table I lists these values along with the degree of polymerization, DP, of the parent polystyrene based on M_w and the corresponding contour length L. We assume a monomer length of 0.252 nm and a DP of the sulfonated polymer equal to that of the parent stock. Also listed are the degree of sulfonation as measured by titration and the corresponding molecular weight of the K-PSS based on the experimentally determined values of d.

We measured the concentrations of salt-free polymer solutions with a Cary 14 spectrophotometer calibrated with standard solutions whose concentrations were determined by dry weight analysis. All optical densities were measured at ~25 °C and a wavelength of 261.5 nm, a strong absorption peak for K-PSS.[9] The optical density varied linearly with concentration throughout the range 10^{-4}–10^{-3} g/mL for all three molecular weights. The extinction coefficient ranged from 1659 cm^2/g for sample 17 to 1682 cm^2/g for sample 25, compared with 1750 cm^2/g for the 100% sulfonated K-PSS reported by Raziel.[9] The optical densities of the calibration standards varied by only ±1% even after 6 months of frozen storage. The K-PSS concentrations were reproducible within 1% from day to day.

Viscometry. We employed Cannon-Ubbelohde size 50 semimicro dilution viscometers, which require only small starting volumes of polymer solution and permit easy serial dilutions. All experiments were performed in a Cannon M1 water bath regulated at 25 ± 0.02 °C. We used single-bulb viscometers for Newtonian solutions and four-bulb viscometers for shear-thinning solutions.

The shear-thinning nature of polyelectrolyte solutions necessitates some extrapolation to the zero-shear limit. The pressure head ρgh driving the flow through the tube of length l and radius R is related to stress by

$$-\eta\frac{dv}{dr} = \frac{\rho ghr}{2l} \qquad (13)$$

We first expand the viscosity and velocity v in powers of

$$\epsilon = \frac{\rho ghR}{2l\eta_0}\tau \ll 1$$

with τ the relaxation time for the polymer solution. Substituting these expansions into (13) yields

$$\frac{1}{\eta_r^{app}} = \frac{1}{\eta_{r0}} + \frac{\tau^2}{6\eta_{r0}^3}\left(\frac{\rho hR}{l\eta_0}\right)^2 h^2 + \frac{3B\tau^4}{32\eta_{r0}^5}\left(\frac{\rho gR}{l\eta_0}\right)^4 h^4 \qquad (14)$$

with η_r^{app} and h the apparent relative viscosity and corresponding head for a particular measurement. The true low shear relative viscosity, η_{r0}, and τ and B, characterizing the shear thinning, are the material parameters of interest which depend on polymer molecular weight and concentration and the ionic strength.

By plotting $(1/\eta_r^{app})$ vs. the height squared, h^2, we obtain a curve with y-intercept $1/\eta_{r0}$. For weakly shear-thinning fluids, $\epsilon \ll 1$, so the data are fitted by the least-squares method to determine τ. More strongly shear-thinning fluids required fitting a quadratic curve, yielding B.

The quadratic extrapolation was necessary only for sample 17 for $I < 3 \times 10^{-3}$ M (e.g., Figure 1). For $I = 7 \times 10^{-3}$ M, the linear and quadratic extrapolations yielded values for $[\eta]$ and k_H that agreed within the typical degree of reproducibility. In Figure 2, the smooth variation of τ^2 for sample 17 vs. c for the three lowest ionic strengths demonstrates the reliability of the extrapolation procedure. For 0.05 M < I < 3.1 M, the solutions were effectively Newtonian, so a single-bulb viscometer sufficed.

For sample 25 at $I = 10^{-3}$ M, linear extrapolation with the top three bulbs in the four-bulb viscometer was sufficient. For 3×10^{-3} M < I < 1.0 M, single-bulb viscometers gave accurate zero-shear data. For sample 24, solutions were effectively Newtonian for all ionic strengths, 10^{-3}–1.0 M.

Dilution Methods. In a series of dilutions to measure $[\eta]$ and k_H, the polymer concentration c and the ionic strength can be varied independently by controlling the ionic strength I of the diluent. We employed isoionic dilution which maintains the total ionic strength, and thus κ^{-1} and L_p, constant. The difficulty is that isoionic dilution requires knowing the contribution of the polymer to the overall ionic strength.

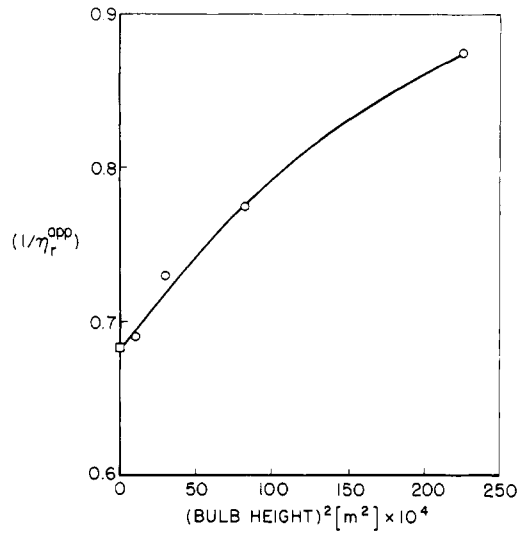

Figure 1. Zero-shear extrapolation for S-17, $I = 3 \times 10^{-5}$ M.

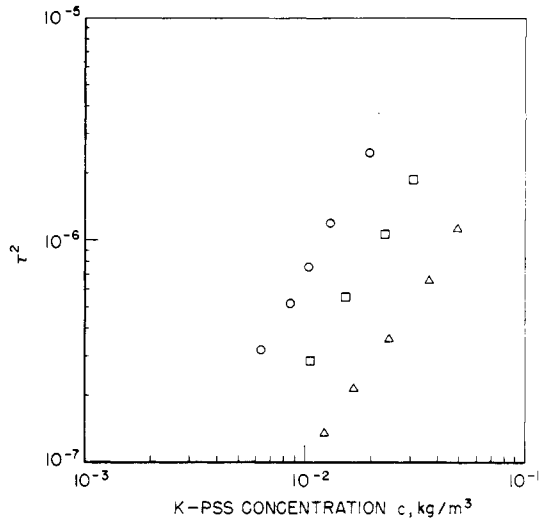

Figure 2. Plot of $\mathcal{O}(\dot{\gamma}^2)$ coefficient $A\tau^2$ vs. polymer concentration for sample 17: (○) $I = 3 \times 10^{-5}$ M; (□) $I = 1 \times 10^{-4}$ M; (△) $I = 3 \times 10^{-4}$ M.

For a polyelectrolyte solution with added salt at ionic strength I_s, the effective ionic strength is

$$I = I_s + \frac{1}{2}\left(\frac{L_B}{L_c}\right)_{eff}\frac{LN_Ac}{L_BM} \tag{15}$$

with $(L/L_B)(L_B/L_c)_{eff}$ representing the number of free counterions per chain and the factor of $^1/_2$ indicating that the fixed charges on the backbone do not contribute.

Pals and Hermans[18] determined $(L_B/L_c)_{eff}$ empirically for cmc as the value giving straight-line plots of η_{sp}/c vs. c. Tereyama and Wall[19] followed a similar procedure for potassium cellulose sulfate. Moan and Wolff[20] on the other hand, estimated $(L_B/L_c)_{eff}$ for cmc from measured values of the osmotic coefficient as suggested by the theory of ref 21.

Here we employ Manning's[22] counterion condensation theory based on the linearized line charge model, which leads to

$$\left(\frac{L_B}{L_c}\right)_{eff} = \frac{L_B}{L_c} \quad \frac{L_B}{L_c} < 1$$
$$= 1 \quad \frac{L_B}{L_c} > 1 \tag{16}$$

Thus for charge spacing greater than L_B the actual and effective charge densities are equal. But for $L_c < L_B$, the intense electric field around the polymer backbone localizes counterions, limiting the effective density to one charge per Bjerrum length L_B.

All three K-PSS samples in the present study had $L_B/L_c > 1$. The error incurred in assuming $(L_B/L_c)_{eff} = 1$ instead of values

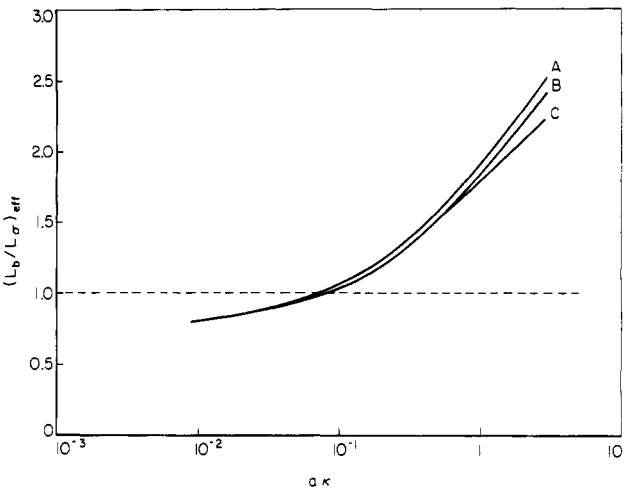

Figure 3. Effective charge density vs. $a\kappa$: (A) sample 25; (B) sample 24; (C) sample 17; (--) Manning's counterion condensation theory.

calculated from the nonlinear model for nonzero $a\kappa$[1] is illustrated in Figure 3 for the range of $a\kappa$ values encountered in this work. At low ionic strengths, $0.009 < a\kappa < 0.1$, where the polymer contributes most to the overall ionic strength, $(L_B/L_c)_{eff}$ varies from 0.8 to 1.05; thus the linearized prediction does not err significantly. The error increases, however, as molarity decreases because a higher initial polymer concentration is needed to reach $\eta_{rel} \sim 1.3$. Nonetheless, for sample 24 at $I > 0.01$ M, the error in the ionic strength remains less than 10%; thus the error in $(L_B/L_c)_{eff}$ never significantly affects the isoionic dilution.

We did not dilute at constant chemical potential of the salt, also known as dialysis dilution, because this method does not maintain a constant ionic strength as the polymer concentration decreases. Neither are the changes in polymer conformation with dilution known. With isoionic dilution the neutron scattering experiments of Moan and Wolff[20] indicate that the persistence length does remain constant. Hence only direct intermolecular interactions should alter the conformation, as with nonionic polymers in good solvents.

The measured intrinsic viscosity is independent of the method of dilution but the Huggins coefficients are not. Pals and Hermans[18] related the Huggins coefficients obtained by isoionic dilution and dilution at constant added salt concentration by differentiating the dilute viscosity equation, eq 1, with respect to ionic strength I. They obtained

$$(k_H)_i = (k_H)_{cs} - \frac{1}{2}\left(\frac{L}{L_c}\right)_{eff}\frac{N_A}{M[\eta]}\frac{d \ln [\eta]}{dI} \tag{17}$$

where the subscripts i and cs refer to the two dilution methods. Since $d \ln \eta/dI$ is negative, $(k_H)_i > (k_H)_{cs}$.

The relation between the Huggins coefficients measured by isoionic dilution and dialysis dilution for a completely substituted chain can be derived similarly as

$$(k_H)_i = (k_H)_d + \left[\frac{\Gamma}{[\eta]}\right]\frac{d \ln [\eta]}{dI} \tag{18}$$

where the subscript d refers to dialysis dilution and $\Gamma > 0$ is the Donnan salt exclusion coefficient.[23] For normal polyelectrolytes, $(k_H)_i > (k_H)_d$.

Figure 4 illustrates data from sample 17 obtained by dilution with deionized water so that the ionic strength changes with polymer concentration. The 7-fold increase in η_{sp}/c as c decreases demonstrates the expansion of the coil as the total ionic strength, solely due to counterions, decreases. Figures 5 and 6 represent isoionic dilutions for samples 17 and 24 at their lowest ionic strengths, 3×10^{-5} and 10^{-3} M, respectively. The small error in dilution due to use of the linear theory caused the slight curvature in the latter. In this extreme case, the K-PSS counterions accounted for approximately 95% of the ionic strength at the highest polymer concentration. All other experiments showed much less curvature.

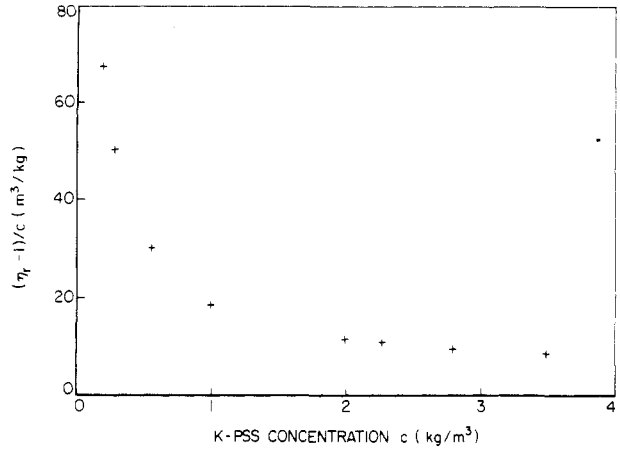

Figure 4. Salt-free dilution viscosity experiment for sample 17, M = 1170.

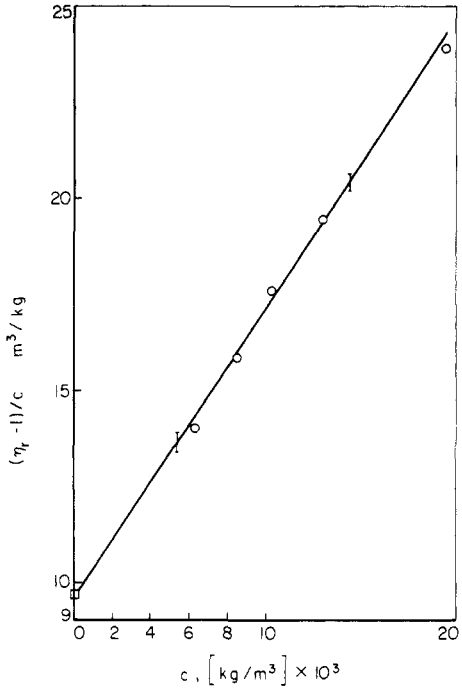

Figure 5. Isoionic dilution of sample 17, M = 1170 at $I = 3 \times 10^{-5}$ M.

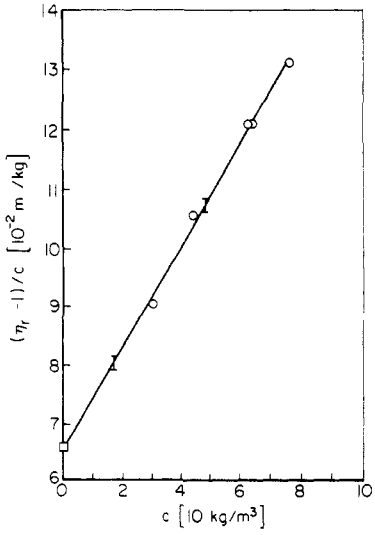

Figure 6. Isoionic dilution for sample 24.

Typical experimental precision was ±3% for $[\eta]$ and ±6% for k_H. Repetition of one-third of the experiments established average reproducibilities of 5% for $[\eta]$ and 20% for k_H. Maximum starting polymer concentrations always satisfied $c[\eta] < 0.3$, confirming the experiments to the dilute regime.[24] Most experiments were conducted in the range $1.05 < \eta_r < 1.3$ to provide typically five data points for the $c \rightarrow 0$ extrapolation.

Table II
Experimental Results

M	I, mol/L	$[\eta]$, mL/g	k_H	$L_p - L_\infty$, Å	$(L_B/L_c)_{eff}$
1.17E+3	3.00E-5	9661.00	7.907	6994.00	0.8061
1.17E+3	1.00E-4	7685.00	3.292	2295.00	0.8415
1.17E+3	3.00E-4	5786.00	1.278	856.4	0.8841
1.17E+3	7.00E-4	3960.00	0.792	414.2	0.9263
1.17E+3	7.00E-4	3948.00	1.006	414.2	0.9263
1.17E+3	1.00E-3	3441.00	0.691	308.9	0.9417
1.17E+3	1.00E-3	3264.00	0.763	308.9	0.9417
1.17E+3	3.00E-3	1858.00	0.590	133.6	1.0263
1.17E+3	7.00E-3	1196.00	0.468	76.30	1.1066
1.17E+3	5.00E-2	486.0	0.266	29.07	1.3819
1.17E+3	5.00E-2	482.5	0.273	29.07	1.3819
1.17E+3	1.00E-1	364.6	0.236	22.56	1.5134
1.17E+3	1.00E-1	356.9	0.275	22.56	1.5134
1.17E+3	3.00E-1	225.3	0.325	15.69	1.7530
1.17E+3	1.00E+0	115.2	0.365	10.45	2.0180
1.17E+3	2.75E+0	31.93	1.47	7.10	2.2024
1.17E+3	3.10E+0	17.17	4.966	6.76	2.2209
1.17E+3	3.10E+0	15.97	4.874	6.76	2.2209
10.95E+1	1.00E-3	147.70	18.700	313.20	0.9555
10.95E+1	3.00E-3	110.00	5.556	135.90	1.0380
10.95E+1	3.00E-3	105.00	6.620	135.90	1.0380
10.95E+1	7.00E-3	83.50	2.930	78.06	1.1218
10.95E+1	5.00E-2	47.60	0.625	30.37	1.4145
10.95E+1	1.00E-1	39.93	0.493	23.81	1.5559
10.95E+1	3.00E01	28.19	0.427	16.86	1.8156
10.95E+1	1.00E+0	15.04	0.792	11.47	2.1136
10.95E+1	1.00E+0	16.35	0.737	11.47	2.1136
4.15E+1	1.00E-3	65.71	20.02	312.60	0.9544
4.15E+1	3.00E-3	35.86	15.09	135.60	1.0360
4.15E+1	3.00E-3	38.96	12.37	135.60	1.0360
4.15E+1	7.00E-3	31.34	4.01	77.78	1.1195
4.15E+1	4.00E-3	29.24	6.74	77.78	1.1195
4.15E+1	1.00E-2	27.50	3.733	63.24	1.1614
4.15E+1	5.00E-2	18.79	1.272	30.16	1.4091
4.15E+1	4.00E-1	15.65	1.144	23.61	1.5485
4.15E+1	1.00E+0	8.33	0.698	11.30	2.1003
4.15E+1	1.00E+0	8.09	0.800	11.30	2.1003

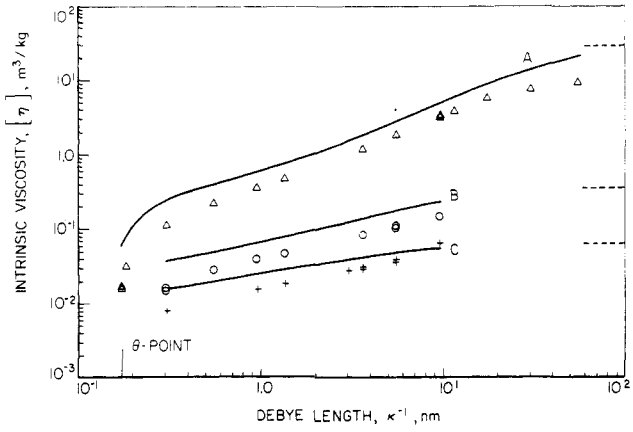

Figure 7. Intrinsic viscosity of K-PSS: (+) sample 24; (○) sample 25; (△) sample 17; (—) Yamakawa model predictions; (– –) rod limits.

Results and Discussion

Intrinsic Viscosities. Our results for $[\eta]$ and k_H for $3 \times 10^{-5} < I < 3.1$ M, corresponding to $0.009 < a\kappa < 2.89$ are listed in Table II and plotted vs. κ^{-1} in Figures 7 and 9. Also listed are calculated values of the electrostatic persistence length $L_e = \hat{G}/(4L_B\kappa^2)$ and the effective charge density $(L_B/L_c)_{eff}$ based on the data in Table I. Note in Figure 7 that, as κ^{-1} increases, $[\eta]$ increases dramatically,

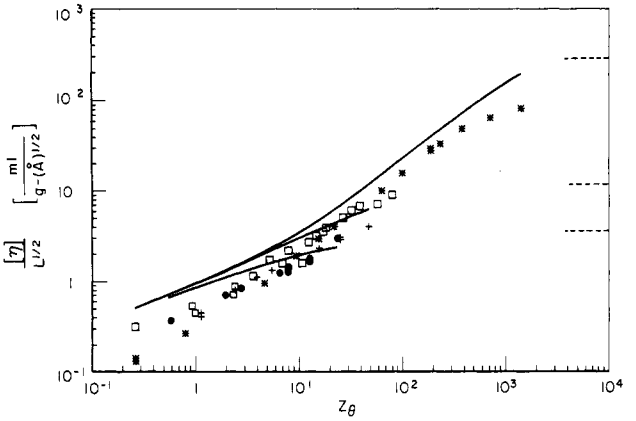

Figure 8. Nondraining intrinsic viscosity correlation: (□) Raziel's data; (●) sample 24; (+) sample 25; (☆) sample 17; (—) nonlinear theory; (– –) rod limit.

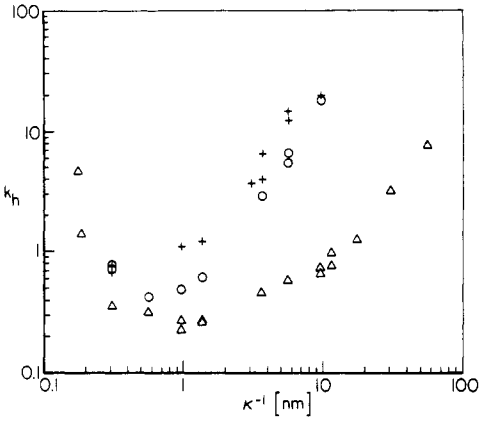

Figure 9. Huggins coefficient of K-PSS: (+) sample 24; (○) sample 25; (△) sample 17.

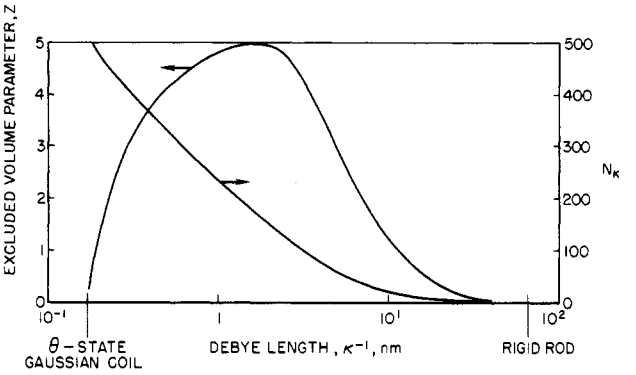

Figure 10. Excluded volume parameter z and number of Kuhn lengths N_k for sample 17, M = 1170.

e.g., over 3 orders of magnitude, for sample 17, clearly demonstrating the important role of electrostatic forces in determining conformation. Near the Θ-point at 3.1 M $[\eta]$ decreases sharply, reflecting the rapid collapse of the chain as the short-range attractions become significant. This overall dependence of $[\eta]$ on ionic strength resembles that seen for many other polyelectrolytes, e.g., poly(acrylic acid).[25]

Figure 7 demonstrates that the combination of the electrostatic and hydrodynamic wormlike chain models reviewed briefly above and described in detail in ref 1 tracks the experimental results quite closely from the nondraining Gaussian coil limit to the rod limit. The theory requires only the parameters in Table I, which were extracted from Raziel's light scattering data and knowledge of the molecular structure. The predictions do err by 50% or more on the high side, but the variation in $[\eta]$ is much larger. We previously demonstrated a similar correspondence with data from one of Raziel's samples.[1]

Figure 7 also displays the rod limits for $[\eta]$ from the wormlike chain theory, the primary electroviscous effect[26] being negligible for these conditions. For sample 24 at 10^{-3} M, $N_k \sim 1.5$ and the experimental value falls below the limit. For samples 25 and 17 $N_k \geq 1$ at the lowest ionic strength, but the data appear to approach the appropriate limits.

The theoretical results discussed above suggest correlating the data for different molecular weights as $[\eta]/L^{1/2}$ vs.

$$z_\theta = 2\left(\frac{3}{2\pi}\right)^{3/2}\left(\frac{L}{L_\infty}\right)^{1/2}\frac{R(w)}{\kappa L_\infty} \qquad (19)$$

which is the excluded volume parameter in the absence of chain stiffening. Figure 8 shows that our data plus that of Raziel's for five molecular weights ranging from 46.7 to 2275 collapse into a single band. The corresponding theoretical curves indicate that the points should diverge as the molecules expand and both internal flow and chain stiffening become significant. For $z_\infty \gg 1$ each molecular weight must approach a different limit with $[\eta] \propto L^3/M$ ln $(2L/a)$ as for rods. Data for sample 17 clearly do and that for sample 25 shows a similar tendency. Thus the correlation illustrates the transition from nondraining to free-draining, or random-coil to extended-rod, behavior.

Huggins Coefficients. The measured Huggins coefficients (Figure 9) have three striking features: (1) high values at low ionic strengths, (2) minima at intermediate ionic strengths, and (3) high values at the Θ-state. In the following we interpret these in terms of the direct contributions of the intermolecular electrostatic force to the stress, the coil compression produced by these same intermolecular forces, and the attractions that appear near Θ-conditions, respectively.

The minima in k_H are apparent for samples 17 and 25 (Figure 9). For the former the value of 0.26 at $I \sim 0.05$ M lies significantly below the free-draining limit of 0.40. As indicated by (11) the contribution of coil compression to k_H depends on the excluded volume parameter z. The plot of z as a function of κ^{-1} in Figure 10 demonstrates that z initially increases rapidly with decreasing ionic strength due to the increase in the binary cluster integral β. Simultaneously, though, N_k decreases as the backbone becomes stiffer. Consequently, the probability of intramolecular segment–segment interactions, embodied in $K(N_k)$, decreases, causing z to pass through a maximum and then decrease. The maximum therefore reflects the opposing effects of segment–segment excluded volume and chain stiffening with the location depending on the structural parameters. Calculations of z based on the theory outlined previously predict the maximum at I = 0.05 M for sample 17, coinciding with the minimum in k_H.

At lower ionic strengths the coil compression decreases and the direct contribution of electrostatic interactions to the viscosity, an $\mathcal{O}(z_\infty^2)$ effect, becomes significant. For the lowest molecular weight, sample 24, no minima was observed, perhaps reflecting the greater magnitude of the direct effect relative to coil compression.

The values greater than 0.76, the limit for nondraining coils, for k_H at the Θ-state apparently arise from intermolecular attractions. Within the context of a two-parameter theory the existence of a Θ-state at finite ionic strength implies sufficient segment–segment attractions to compensate for the electrostatic repulsion and make z = 0. Then the theory predicts the second virial coefficient

Table III

MW	I, M	L_k, Å	N_k	Z	α_t	[η], mL/g exptl	[η], mL/g theor	f_0, g/s	$1/\kappa R_g$	A_2, cm³·mol/g²	k_H	$(k_h - 0.4)/[6\pi\eta_0 R_g/f_0]$
0.1170E+07	0.300E-04	12554.94	1.14	0.002	13.13	9661.00	22032.62	0.153E-05	0.1636	0.255E+00	7.9070	2.0127
0.1170E+07	0.100E-03	4344.32	3.29	0.086	10.62	7685.00	14274.54	0.146E-05	0.1108	0.106E+00	3.2920	0.9164
0.1170E+07	0.300E-03	1671.23	8.56	0.415	8.27	5786.00	8776.85	0.135E-05	0.0821	0.388E-01	1.2780	0.3302
0.1170E+07	0.700E-03	825.13	17.34	0.964	6.68	3960.00	5759.64	0.124E-05	0.0665	0.176E-01	0.7920	0.1671
0.1170E+07	0.700E-03	825.13	17.34	0.964	6.68	3948.00	5759.64	0.124E-05	0.0665	0.176E-01	1.0060	0.2583
0.1170E+07	0.100E-02	621.21	23.03	1.293	6.10	3441.00	4785.51	0.118E-05	0.0610	0.127E-01	0.6910	0.1301
0.1170E+07	0.100E-02	621.21	23.03	1.293	6.10	3264.00	4785.51	0.118E-05	0.0610	0.127E-01	0.7630	0.1623
0.1170E+07	0.300E-02	278.91	51.29	2.675	4.65	1858.00	2701.67	0.102E-05	0.0462	0.497E-02	0.5900	0.0959
0.1170E+07	0.700E-02	166.05	86.15	3.855	3.84	1196.00	1765.74	0.901E-06	0.0366	0.260E-02	0.4680	0.0368
0.0070E+07	0.500E-01	72.47	197.39	4.955	2.67	486.00	757.11	0.689E-06	0.0197	0.798E-03	0.2660	-0.0799
0.1170E+07	0.500E-01	72.47	197.39	4.955	2.67	482.50	757.11	0.689E-06	0.0197	0.798E-03	0.2730	-0.0757
0.1170E+07	0.100E+00	59.52	240.35	4.765	2.40	364.60	592.02	0.634E-06	0.0155	0.575E-03	0.2360	-0.0998
0.1170E+07	0.100E+00	59.52	240.35	4.765	2.40	356.90	592.02	0.634E-06	0.0155	0.575E-03	0.2750	-0.0761
0.1170E+07	0.300E+00	45.83	312.16	4.278	2.07	225.30	416.40	0.560E-06	0.0104	0.361E-03	0.3250	-0.0468
0.1170E+07	0.100E+01	35.37	404.48	3.083	1.72	115.20	255.35	0.477E-06	0.0068	0.203E-03	0.3650	-0.0224
0.1170E+07	0.275E+01	28.68	498.89	0.486	1.20	31.93	99.61	0.343E-06	0.0059	0.492E-04	0.4700	0.7068
0.1170E+07	0.310E+01	28.00	511.00	0.019	1.01	17.17	63.16	0.292E-06	0.0066	0.325E-05	4.9660	3.0452
0.1170E+07	0.310E+01	28.00	511.00	0.019	1.01	15.97	63.16	0.292E-06	0.0066	0.325E-05	4.8740	2.9839
0.1095E+06	0.100E-02	517.14	2.51	0.112	3.51	147.70	226.69	0.193E-06	0.3521	0.258E-01	18.7000	7.6989
0.1095E+06	0.300E-02	255.28	5.08	0.408	3.06	110.00	174.49	0.184E-06	0.2333	0.992E-02	5.5560	2.3722
0.1095E+06	0.300E-02	255.28	5.08	0.408	3.06	105.00	174.49	0.184E-06	0.2333	0.992E-02	6.6200	2.8617
0.1095E+06	0.700E-02	158.94	8.17	0.699	2.69	83.50	137.56	0.174E-06	0.1736	0.510E-02	2.9300	1.2526
0.1095E+06	0.500E-01	73.52	17.65	1.037	2.02	47.60	77.08	0.149E-06	0.0867	0.152E-02	0.6250	0.1274
0.1095E+06	0.100E+00	61.16	21.22	1.016	1.85	39.93	64.69	0.141E-06	0.0669	0.108E-02	0.4930	0.0544
0.1095E+06	0.300E+00	47.82	27.14	0.926	1.63	28.19	49.95	0.130E-06	0.0439	0.669E-03	0.4270	0.0165
0.1095E+06	0.100E+01	37.28	34.82	0.702	1.39	15.04	36.63	0.116E-06	0.0280	0.370E-03	0.7920	0.2495
0.1095E+06	0.100E+01	37.28	34.82	0.702	1.39	16.35	36.63	0.116E-06	0.0280	0.370E-03	0.7370	0.2145
0.4150E+05	0.100E-02	329.24	1.50	0.036	2.36	65.71	53.50	0.911E-07	0.8479	0.301E-01	20.0200	9.3930
0.4150E+05	0.300E-02	204.51	2.41	0.138	2.21	35.86	46.84	0.891E-07	0.5232	0.133E-01	15.0900	7.3508
0.4150E+05	0.300E-02	204.51	2.41	0.138	2.21	38.96	46.84	0.891E-07	0.5232	0.133E-01	12.3700	5.9898
0.4150E+05	0.700E-02	139.49	3.54	0.273	2.06	31.34	41.42	0.868E-07	0.3669	0.700E-02	4.0100	1.8852
0.4150E+05	0.700E-02	139.49	3.54	0.273	2.06	29.24	41.42	0.868E-07	0.3669	0.700E-02	6.7400	3.3109
0.4150E+05	0.100E-01	120.18	4.11	0.329	1.99	27.50	38.86	0.856E-07	0.3177	0.544E-02	3.7330	1.7759
0.4150E+05	0.500E-01	70.37	7.01	0.465	1.69	18.79	28.21	0.790E-01	0.1680	0.205E-02	1.2720	0.5070
0.4150E+05	0.100E+00	59.25	8.33	0.469	1.57	15.65	24.13	0.760E-07	0.1273	0.145E-02	1.1440	0.4464
0.4150E+05	0.100E+01	36.71	13.44	0.345	1.24	8.33	15.29	0.655E-07	0.0510	0.469E-03	0.6980	0.1951
0.4150E+05	0.100E+01	36.71	13.44	0.345	1.24	8.09	15.29	0.655E-07	0.0510	0.469E-03	0.800	0.2619

to be zero and the viscosity to be determined by the hydrodynamic interactions alone. For these solutions, that appears not to be true. Although we have no alternative model, the results available for adhesive spheres[27] are suggestive. These consist of impenetrable spheres with an attractive interaction of zero range, i.e., a stickiness, which produces a population of doublets in equilibrium with pairs not in contact. When the stickiness is sufficient to produce a zero second virial coefficient in the osmotic pressure, the Huggins coefficient equals ~2.3, comparable to that observed here, suggesting that the Θ-state may not be an ideal random coil for these molecules. Coupled with the anomalous value for the Flory coefficient Φ_∞ discussed in ref 1, this provides evidence for the inadequacy of the two-parameter theory in describing these solutions at high ionic strengths.

At low ionic strengths beyond the minima the increase in k_H resembles the secondary electroviscous effect observed with charged particles such as polystyrene latices.[28] The magnitude of that effect is a sensitive function of the range of the interparticle repulsion relative to the particle size, suggesting a correlation of our data, eq 12, as $(k_H - 0.40)f_0/6\pi\eta_0 R_g$ vs. $1/\kappa R_g$. This involves using the various theories to predict f_0 and α_τ as given in Table III. The results for the scaled increment in the Huggins coefficient plotted in Figure 11 vary roughly as $(\kappa R_g)^{-2}$ as suggested by the general form of (12). Unfortunately, substitution of the $\bar{z}$ calculated for the three samples into (12) produces the solid curves, which deviate substantially from the data. The discrepancy may simply reflect the effect of coil compression or alternatively a failure of the smoothed density or free-draining assumptions in the theory for the direct contributions to the stress.

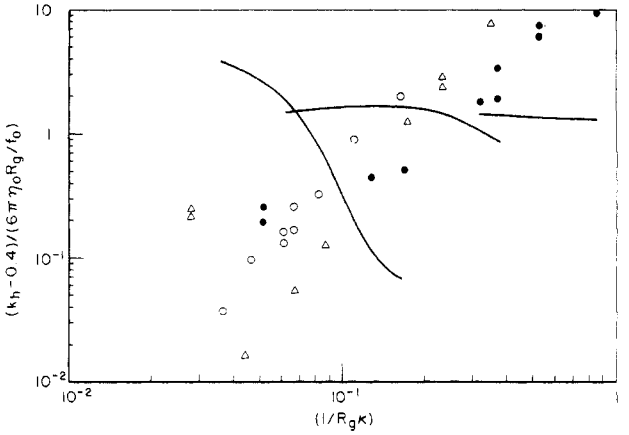

Figure 11. Scaled Huggins coefficient plot: (●) sample 24; (△) sample 25; (○) sample 17; (—) Russel's theory.

Summary

Our intrinsic viscosity measurements on a series of well-characterized monodisperse K-PSS samples span conformations from rodlike at low ionic strength to Gaussian coils at high ionic strength. The electrostatic wormlike chain theory coupled with a corresponding theory for the hydrodynamics tracks the intrinsic viscosity semiquantitatively over 3 orders of magnitude. Alternatively, a correlation based on nondraining hydrodynamics reduces the data from K-PSS samples of several molecular weights and illustrates the consequences of the conformational transition.

The measured Huggins coefficients show minima due to coil compression by intermolecular interactions that correlate with the excluded volume parameter z. Unexpectedly high values of the Huggins coefficient near the Θ-state of K-PSS are attributed to short-range attractive forces that affect both inter- and intramolecular behavior. Even larger values of the Huggins coefficient at low ionic strengths arise from intermolecular interactions as for charged polymer latices. Existing theory, however, fails to predict the magnitudes accurately.

Acknowledgment. This work was supported by the National Science Foundation through Grant ENG-7825929.

References and Notes

(1) Davis, R. M.; Russel, W. B. *J. Polym. Sci., Polym. Phys. Ed.* **1986**, *24*, 511.
(2) Odijk, T. *J. Polym. Sci., Polym. Phys. Ed.* **1977**, *15*, 477.
(3) Odijk, T. *Polymer* **1978**, *19*, 989.
(4) Odijk, T.; Houwaart, A. C. *J. Polym. Sci., Polym. Phys. Ed.* **1978**, *16*, 627.
(5) Skolnick, J.; Fixman, M. *Macromolecules* **1977**, *10*, 944.
(6) Fixman, M.; Skolnick, J. *Macromolecules* **1978**, *11*, 863.
(7) Fixman, M. *J. Chem. Phys.* **1982**, *76*, 6346.
(8) Yamakawa, H.; Fujii, M. *Macromolecules* **1974**, *7*, 128.
(9) Raziel, A.; Eisenberg, H. *Isr. J. Chem.* **1973**, *11*, 183.
(10) Yamakawa, H. *Modern Theory of Polymer Solutions*; Harper and Row: New York, 1971.
(11) Yamakawa, H.; Stockmayer, W. *J. Chem. Phys.* **1972**, *57*, 2843.
(12) Yamakawa, H.; Tanaka, G. *J. Chem. Phys.* **1967**, *47*, 3991.
(13) Batchelor, G. K. *J. Fluid Mech.* **1977**, *83*, 97.
(14) Saito, N. *J. Phys. Soc. Jpn.* **1952**, *7*, 447.
(15) Freed, K. F.; Edwards, S. F. *J. Chem. Phys.* **1975**, *62*, 4032.
(16) Muthukumar, M.; Freed, K. F. *Macromolecules* **1977**, *10*, 899.
(17) Russel, W. B. *J.* Fluid *Mech.* **1979**, *92*, 401.
(18) Pals, D. T. F.; Hermans, J. J. *Recl. Trav. Chim. Pays-Bas* **1952**, *71*, 433.
(19) Tereyama, H.; Wall, F. T. *J. Polym. Sci.* **1955**, *16*, 357.
(20) Moan, M.; Wolff, C. *Polymer* **1975**, *16*, 776.
(21) Katchalsky, A.; Lifson, S. *J. Polym. Sci.* **1956**, *11*, 409.
(22) Manning, G. S. *J. Chem. Phys.* **1969**, *51*, 924.
(23) Russel, W. B. *J. Polym. Sci., Polym. Phys. Ed.* **1982**, *20*, 1233.
(24) Graessley, W. *Adv. Polym. Sci.* **1982**, *47*, 67.
(25) Lapanje, S.; Kovac, S. *J. Macromol. Sci., Chem.* **1967**, *A1*, 707.
(26) Sherwood, J. D. *J. Fluid Mech.* **1981**, *111*, 347.
(27) Russel, W. B. *J. Chem. Soc., Faraday Trans. 1* **1984**, *80*, 31.
(28) Stone-Masui, J.; Watillon, A. *J. Colloid Interface Sci.* **1968**, *28*, 187.

On the Universality of Viscoelastic Properties of Entangled Polymeric Systems

Kunihiro Osaki,* Eiichi Takatori, Yoshisuke Tsunashima, and Michio Kurata

Institute for Chemical Research, Kyoto University, Uji, Kyoto 611, Japan.
Received August 20, 1986

ABSTRACT: Viscoelastic properties were examined for solutions with various molecular weights, M, and concentrations, c, of poly(α-methylstyrene) and polystyrene in chlorinated biphenyl. The number of entanglements per molecule, N, was evaluated from the plateau modulus, G_N. The longest relaxation time, τ_1, was evaluated from the relaxation modulus, $G(t)$; the relaxation time of an entanglement strand, τ_s, was evaluated from the complex modulus in the glass-to-rubber transition region; and another time constant, τ_k, was defined as the time at which the quantity $G(t,\gamma)/G(t)$ levels off, where $G(t,\gamma)$ is the relaxation modulus at a finite magnitude of shear, γ. Reduced storage and loss moduli, $G'(\omega)/G_N$ and $G''(\omega)/G_N$, regarded as functions of reduced angular frequency, $\omega\tau_s$, were determined if the number N was given, irrespective of the combinations of M and c or of the polymer species. The same held true for a nonlinear function, $G(t,\gamma)/G(t)$, regarded as a function of γ and reduced time, t/τ_s. The ratios τ_1/τ_s and τ_k/τ_s were unique functions of N for all the solutions studied and were proportional to $N^{3.5}$ and $N^{2.0}$, respectively. The magnitudes of these ratios were in accord with the interpretation that τ_1 corresponds to the reptation time and τ_k to the time for complete equilibration of the fluctuation of chain contour length in the tube model theory.

Introduction

According to the current concept of polymer entanglement,[1,2] two polymeric systems having an identical number of entanglements per molecule, N, should exhibit a common viscoelastic behavior in the sense that the shape of the curve corresponding to log (viscoelastic function) plotted against log t or log ω is the same. Here t is the time and ω is the angular frequency. The quantity N is written as

$$N = M/M_e \tag{1}$$

where M is the molecular weight and M_e is the entanglement molecular weight. The latter is determined from the rubbery plateau modulus, G_N, through

$$G_N = cRT/M_e \tag{2}$$

where c is the mass concentration, R is the gas constant, and T is the absolute temperature. Thus for a system with a given M and c, the shape of a viscoelastic function in appropriate scales will be determined by a scale unit, G_N, for the viscoelastic modulus functions such as the relaxation modulus and the complex modulus. Two systems with different combinations of M and c will show the same viscoelastic behavior in appropriately reduced scales provided that the value of N evaluated from M and G_N is the same. This statement was revealed to be true for the linear as well as nonlinear viscoelasticity of a series of polystyrene (PS) solutions. The purpose of the present study is to examine if it is also true over different polymer species.

The observations for PS solutions[3-5] may be summarized as follows. In the glass-to-rubber transition region, the storage modulus, $G'(\omega)$, and the loss modulus, $G''(\omega)$, for samples with various M and c could be described with universal functions, g_A' and g_A'', and two parameters, G_N and τ_s, as

$$G'(\omega) = G_N g_A'(\omega\tau_s) \tag{3a}$$

$$G''(\omega) = G_N g_A''(\omega\tau_s) \tag{3b}$$

0024-9297/87/2220-0525$01.50/0